

# Face2Face: Label-driven Facial Retouching Restoration

Guanhua Zhao\*  
Shenzhen Graduate School, Peking  
University  
Shenzhen, China  
chiukw@stu.pku.edu.cn

Yu Gu\*  
Shenzhen Graduate School, Peking  
University  
Shenzhen, China  
2201212799@stu.pku.edu.cn

Xuhan Sheng  
Shenzhen Graduate School, Peking  
University  
Shenzhen, China  
llstela.sxh@gmail.com

Yujie Hu  
Shenzhen Graduate School, Peking  
University  
Shenzhen, China  
hhuyujie@stu.pku.edu.cn

Jian Zhang<sup>†</sup>  
Shenzhen Graduate School, Peking  
University  
Shenzhen, China  
zhangjian.sz@pku.edu.cn

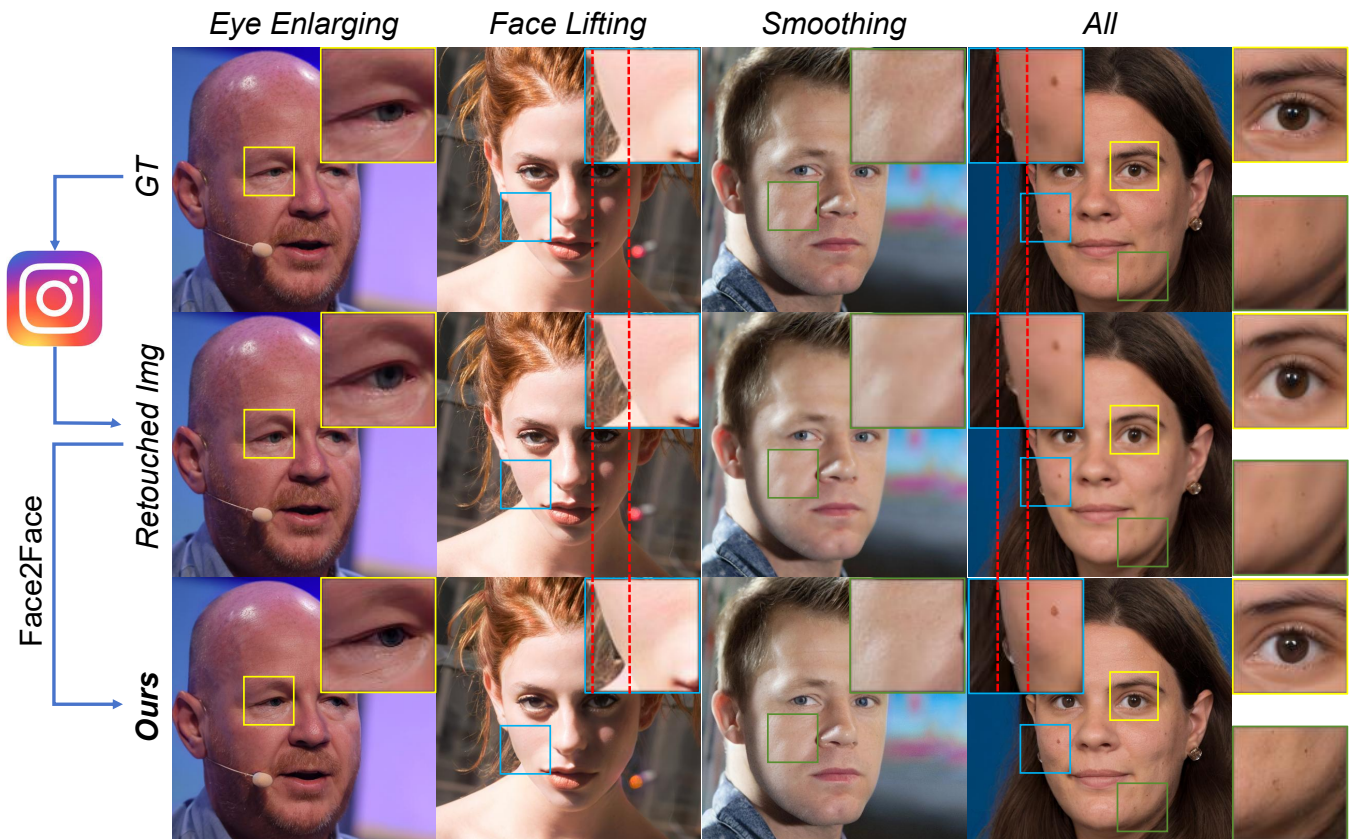


Figure 1: We propose Face2Face, a framework designed to restore the retouched facial image following the retouching label. The original images, denoted as GT, are retouched via photo editing applications such as Instagram, resulting in the Retouched Images. Subsequently, our framework Face2Face is capable of restoring Retouched Images to their original state. The upmost captions indicate the retouching methods employed, with the term "all" denoting the retouching application of three methods. The red dashed line is convenient for observing face lifting.

## ABSTRACT

With the popularity of social media platforms such as Instagram and TikTok, and the widespread availability and convenience of

retouching tools, an increasing number of individuals are utilizing these tools to beautify their facial photographs. This poses challenges that place high demands on the authenticity of photographs, such as identity verification and social media. By altering facial images, users can easily create deceptive images, leading to the dissemination of false information. This may pose

\*Both authors contributed equally to this research.

<sup>†</sup> Corresponding author

challenges to the reliability of identity verification systems and social media, and even lead to online fraud. To address this issue, some work has proposed makeup removal methods, but they still lack the ability to restore images involving geometric deformations caused by retouching. To tackle the problem of facial retouching restoration, we propose a framework, dubbed Face2Face, which consists of three components: a facial retouching detector, an image restoration model named FaceR, and a color correction module called Hierarchical Adaptive Instance Normalization (H-AdaIN). Firstly, the facial retouching detector predicts a retouching label containing three integers, indicating the retouching methods and their corresponding degrees. Then FaceR restores the retouched image based on the predicted retouching label. Finally, H-AdaIN is applied to address the issue of color shift arising from diffusion models. Extensive experiments demonstrate the effectiveness of our framework and each module.

## CCS CONCEPTS

• **Computing methodologies** → **Computer vision.**

## KEYWORDS

Deep Learning, Image Restoration, Face Retouching Restoration

## 1 INTRODUCTION

In contemporary society, we witness the increasing prevalence of photo editing tools and techniques, enabling virtually anyone to digitally construct a version of themselves closer to their ideals with a simple click or swipe [29]. From social media to personal avatars, features such as enlarging eyes, smoothing skin, and slimming faces make facial retouching extremely convenient, turning retouched facial photos into a cultural phenomenon. Undeniably, photo editing technology plays a positive role in satisfying people’s pursuit of beauty and shaping personal brands. However, when retouched photos are applied in contexts requiring authenticity and accuracy, issues arise. Specifically, in fields such as judicial crime investigation, financial services, and security supervision, facial recognition-based identity verification systems are widely used. However, if the provided facial images have been retouched, they may pose a threat to the system’s accuracy, resulting in erroneous identity confirmation and introducing security risks. [7] points out the impact of makeup operations on automatic facial recognition. Similarly, in online social platforms involving interpersonal trust, excessively retouched photos may violate the principles of honest communication, leading to social issues such as identity fraud.

In the current research and technological development, the primary objective of facial retouching detection technology is to classify facial photographs to determine whether they have undergone retouching processing [1, 27, 28, 33, 39]. However, these technologies currently only detect whether a photo has been retouched, without being able to determine the specific retouching methods and their degrees, which to a certain extent limits their applicability. Suppose in an identity verification system, we employ facial retouching detection technology to determine whether the photo uploaded by the user has undergone retouching processing. If the detection result indicates that the photo has been retouched, the system can reject the photo and request the user to upload a new

one. Although this method can help improve the accuracy and reliability of identity verification, it requires users to upload photos multiple times, increasing the complexity of the operation and inconvenience to the user experience. Therefore, if we could adopt more advanced facial retouching restoration technology, we could directly use the retouched photo for identity verification without requiring users to upload it again. The application of this technology will simplify the identity verification process, enhance user experience, help reduce misjudgments, and improve the reliability of the system. Therefore, the development of facial retouching restoration technology holds significant practical significance and application prospects.

Facial retouching restoration aims to revert images that have undergone retouching processes using software such as Photoshop or Meitu to their original states. The range and intensity of retouching methods applied by different software and users vary widely, making it difficult to precisely control the range and intensity of restoration involving retouching methods such as facial lifting and eye enlargement, posing significant challenges for the restoration task. Another significant challenge is that, unlike makeup, retouching operations involve facial geometric transformations while maintaining consistency in facial features. Existing restoration works (Chen et al., 2017; Zheng et al., 2013; Liu et al., 2014) only deal with the reversal of known or linear non-deformation operations.

To tackle these challenges, we propose Label-driven Facial Retouching Restoration (Face2Face), including a facial retouching detector, an image restoration model named FaceR, and a color correction module called Hierarchical Adaptive Instance Normalization (H-AdaIN).

Firstly, we employ a facial retouching detector capable of identifying the retouching methods and degrees presented in retouched images. RetouchingFFHQ [41] introduces a dataset containing over 500,000 conditioned retouched images with large-scale, high-quality, and high-granularity features, along with a novel facial retouching detector (DenseNet121-MAM) capable of analyzing and identifying the methods and degrees of facial retouching in images, rendering the aforementioned task feasible. As the first endeavor on facial restoration from deformation retouching, we select a modest ensemble of retouching techniques, comprising eye enlargement, face lifting, and smoothing. The facial retouching detector predicts a retouching label containing three integers, indicating the retouching methods employed and their corresponding degrees.

Then, the face restoration network (FaceR) restores the retouched image based on the retouching label predicted by the facial retouching detector. [37] points out that pre-trained models on large-scale image datasets excel in extracting image features and maintaining consistency in image-to-image tasks. The Latent Diffusion Models (LDM) [30] trained on the large-scale image dataset ImageNet [32] possess rich pre-trained priors and high-quality generation characteristics. Utilizing LDM, we are able to ensure the fidelity and consistency of the restored images. In order to manipulate the image restoration process using the retouching label predicted by the facial retouching detector, we may directly employ the label as a condition to control the denoising process of LDM. However, the direct fine-tuning of LDM may compromise its robust image priors, thereby impairing the restoration outcomes. Consequently,

we suggest training an additional module ControlNet, while keeping the LDM frozen. The retouching label are exclusively used as conditions within ControlNet.

Additionally, we observe color distribution shifts in the generated restored images, which is also mentioned in [6]. Adaptive Instance Normalization (AdaIN) [17], initially proposed for image style transfer, has subsequently been employed in subsequent works [5, 40] to control color and stylistic consistency in images. AdaIN extracts the mean and variance of pixels from an entire source image and then applies these statistical parameters to adjust the distribution of pixels in a target image. However, we find that simply applying AdaIN to the entire image is not effective in addressing the issue of color shift. Therefore, we propose Hierarchical Adaptive Instance Normalization (H-AdaIN), which extends global adaptive normalization to hierarchical adaptive normalization computations, enabling faithful color restoration of generated images to match the original images’ colors.

We conduct extensive empirical validation, demonstrating the effectiveness of our method Face2Face in achieving significant restoration quality while preserving facial detail consistency. Additionally, the introduction of H-AdaIN provides a new paradigm for color correction, enabling effective correction even in areas with significant local color deviations. Our contributions can be summarized as follows:

1. We propose a framework, Face2Face, which employs retouching labels generated by facial retouching detector as conditions to accomplish facial retouching restoration. Furthermore, to the best of our knowledge, our Face2Face represents the first endeavor to realize facial restoration from deformation retouching.
2. We introduce Hierarchical Adaptive Instance Normalization (H-AdaIN), effectively addressing color shift issues arising from diffusion models.
3. Extensive analysis and experiments prove the effectiveness of our framework and each module.

## 2 RELATED WORK

We conduct a literature review on makeup removal, pinpointing limitations in current methods for makeup removal. Subsequently, we compare different facial retouching detection methods. Finally, we delve into the discussion of diffusion models.

### 2.1 Makeup Removal

Makeup removal is the task of recovering the original facial appearance from facial images with makeup while maintaining consistency. Chen et al. [4] propose a component-based convolution neural network architecture for blind inversion of retouching operations. Li et al. [23] integrate global domain-level loss and local instance-level loss into a dual-input or output GAN network (BeautyGAN) for makeup transfer and removal. Gu et al. [12] introduce a Local Adversarial Disentangling Network (LADN) for facial makeup and makeup removal. Liu et al. [24] propose PSGAN++, which utilizes a makeup distillation network and an identity extraction network for makeup transfer and removal. Sun et al. [35] introduce a Unified Symmetric Semantic-Aware Transformer (SSAT) network, which combines semantic correspondence learning to achieve makeup transfer and removal. The aforementioned works

can only handle non-deformative makeup removal tasks and are not applicable to retouching restoration tasks involving deformations.

### 2.2 Facial Retouching Detection

Bharati et al. [1] employ a Supervised Restricted Boltzmann Machine (SRBM)-based algorithm to classify facial images as either original or retouched, while Sharma et al. [33] propose an improvised patch-based deep convolution neural network (IPDCN2) for the same purpose. Rathgeb et al. [27] conduct a qualitative assessment of retouching applications, utilizing Photo Response Non-Uniformity (PRNU) to distinguish between authentic and retouched images. Jain et al. [18] introduce a hierarchical approach named Digital Alteration Detection using Hierarchical Convolution Neural Network (DAD-HCNN) to differentiate retouched images and original ones. These works can only detect whether an image has been retouched or not, but cannot detect the specific methods and degrees of retouching. [28] proposes a differential facial retouching detection system, which processes pairs of potential reference images of retouched single portraits and corresponding unretouched probe images to detect whether an image has been retouched. [39] is based on a multi-frame dynamic facial detection method. Additionally, there are specialized detection networks designed to detect retouched images [19], as well as detect occluded faces [11].

### 2.3 Diffusion Models

Starting from the proposal of the denoising diffusion probabilistic models by Ho et al. [14], diffusion models have garnered widespread attention and development in the field of image generation. Song et al. [34] propose a significant reduction in the sampling process, thereby improving the model’s generation speed. Dhariwal et al. [8] utilize classifier gradients to guide the diffusion model during sampling, achieving generation quality superior to the state-of-the-art image generation model, BigGAN [2], at the time. The LDM [30] transforms images from the pixel domain to the latent space, significantly reducing computational costs.

Some works efficiently fine-tune diffusion models to accomplish their target tasks. For instance, [10] utilizes text embeddings to guide personalized generation, while [22] notes that fine-tuning a small number of parameters in the cross-attention layer can personalize pre-trained models. In addition to direct fine-tuning of the original network, there are adapter-based fine-tuning methods. [42] suggests freezing the weights of the original U-Net [31] and leveraging an additional U-Net-like structure as an adapter to integrate new features conditioned on text or images into the model. [25] shares the same objective as ControlNet but adopts a different implementation approach. T2I-Adapter [25] integrates features generated by the adapter into the encoder of the U-Net, while ControlNet integrates them into the decoder.

## 3 METHOD

We introduce a novel approach – Face2Face, to address the facial retouching restoration task. Face2Face is composed of three parts: 1) a pre-trained facial retouching detector; 2) an image restoration model – FaceR, which is composed of a pre-trained LDM with fixed parameters and a trainable ControlNet [42]; 3) a color correction module – Hierarchical Adaptive Instance Normalization (H-AdaIN).

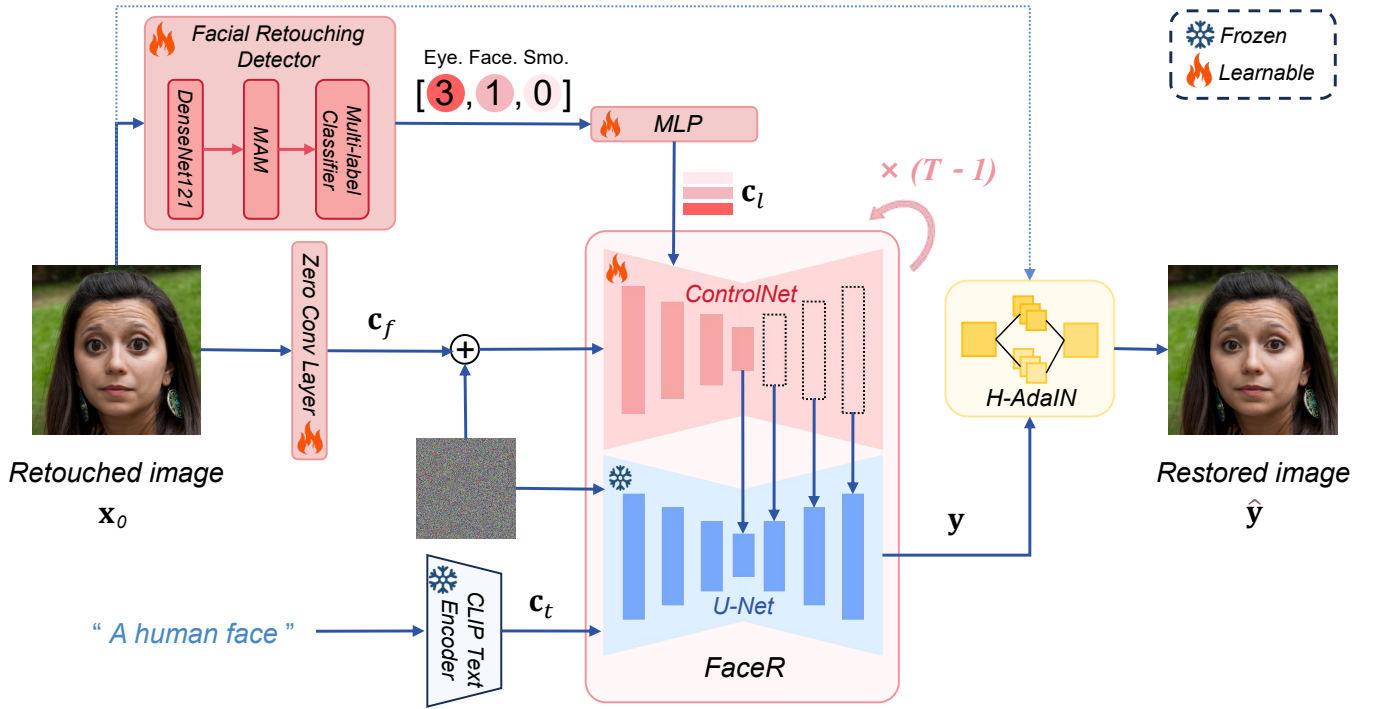


**Figure 2: Overall framework of the proposed Face2Face. The overall architecture is composed of three parts: 1) a pre-trained facial retouching detector; 2) an image restoration model – FaceR, which is composed of a pre-trained LDM with fixed parameters and a trained ControlNet [42]; 3) a color correction module – Hierarchical Adaptive Instance Normalization (H-AdaIN).**

Our framework utilizes retouching labels generated by a facial retouching detector as conditions for restoring retouched images (as elaborated in Sec. 3.1). As depicted in Figure 2, we first employ a facial retouching detector to obtain the retouching label. Then, we input the retouching label and the retouched image into FaceR to obtain the restored image. Further details and the implementation of the FaceR will be elaborated in Sec. 3.2. Finally, the restored image undergoes color correction using the H-AdaIN module to match the color distribution of the original image. The design details and implementation of our H-AdaIN are elaborated in Sec. 3.3.

### 3.1 Facial Retouching Detector

In the task of retouched image restoration, in order to accurately restore the retouched image, it is necessary to detect the retouching methods and their corresponding degrees, so that the restoration network, FaceR, can follow the guidance of the detection results for restoration, rather than blindly restoring. In Sec. 2.2, we discuss relevant retouching detection methods. Considering that our task requires fine-grained detection of retouching methods and degrees, we choose DenseNet121-MAM [41], as shown in Fig. 2. It is an adaptive token clustering method based on multi-layer CNN networks – DenseNet121 [16]. It utilizes attention mechanisms and Gumble Softmax [20] to perform token clustering and reduce spatial redundancy through mean projection. Subsequently, a light-weight two-layer Transformer encoder is introduced to analyze and compare multi-granularity information for enhanced multi-granularity representation learning. Finally, a multi-granularity

attention mechanism is adopted to connect reduced token structures and predict different levels of retouching operations through a multi-label classifier. The entire detection process can be defined as follows:

$$\mathbf{m}_l = FRD(\mathbf{x}_0), \quad (1)$$

where  $\mathbf{m}_l$  represents a retouching label with dimensions  $1 \times 3$ , while  $\mathbf{x}_0$  denotes the input retouched image. For the input  $\mathbf{x}_0$ , it needs to undergo a reshaping operation to adjust its resolution to  $512 \times 512$ , followed by scaling the pixel values from the range of 0-255 to 0-1.

### 3.2 FaceR

FaceR is a key component of the framework Face2Face, aiming to accurately restore a retouched image based on the retouching label  $\mathbf{m}_l$ . One method of fine-tuning neural networks is to directly continue training them, including LDM, using additional training data. However, this approach may result in overfitting and catastrophic forgetting, thereby undermining the robust image priors of the LDM and consequently degrading the quality of the restored images. Therefore, we employ ControlNet to learn the restoration of retouched images, while also leveraging the rich prior knowledge provided by LDM to generate high-quality images. Thus, our FaceR is composed of ControlNet [42] and LDM [30].

LDM is a two-stage diffusion model consisting of an autoencoder and a U-Net noise predictor. In the first stage, LDM trains an autoencoder ( $\mathcal{E}$ ) capable of transforming pixel-space images into latent code  $\mathbf{z}_0 = \mathcal{E}(\mathbf{x}_0)$  and decoding them back into pixel space through

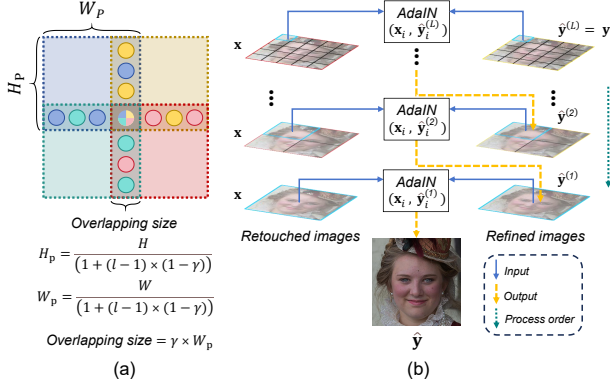


**Figure 3: Hierarchical Adaptive Instance Normalization (H-AdaIN).** (a) The formula for overlapping patches. (b) Overview of H-AdaIN. At level  $l$ , each pair of corresponding  $i^{th}$  patches  $(x_i, y_i^l)$  from  $x$  and  $y^l$  are input into AdaIN. After this, the current refined result  $y^{l-1}$  is obtained, which is used as input at the next level  $l-1$ . The process order of AdaINs is performed from the finest level  $L$  to the coarsest level 1.

the decoder. In the second stage, LDM trains an improved U-Net denoiser to directly denoise in the latent space. The optimization process can be defined by the following equation:

$$\mathcal{L} = \mathbb{E}_{z_t, C, t, \epsilon \sim \mathcal{N}(0, I)} (\|\epsilon - \epsilon_\theta(z_t, t, C)\|_2^2), \quad (2)$$

where  $z_t$  represents the noise sample of  $z_0$  after  $t$  time steps,  $\epsilon$  denotes the noise feature map at time step  $t$ ,  $C$  denotes the control information, and  $\epsilon_\theta$  represents the function of the U-Net denoiser, used to predict the noise added to  $z_t$ . During inference, deterministic DDIM sampling is employed to denoise the stochastic noise  $z_t$  into the latent code  $z_0$ , which is then decoded into the pixel domain  $\hat{x}_0$  through the VAE Decoder. At each time step  $t$ , to balance sample quality and conditional alignment, a classifier-free guidance method [15] is utilized.

$$\tilde{\epsilon}_\theta(z_t, t, C) = (1 + \omega)\epsilon_\theta(z_t, t, C) - \omega\epsilon_\theta(z_t, t), \quad (3)$$

where  $\tilde{\epsilon}_\theta$  represents the score guided by the classifier, used to update  $z_t$  towards  $z_{t-1}$ .  $\omega$  is a scalar controlling the strength of the guidance by  $C$ . The ControlNet is a trainable copy of the encoder block and middle block of U-Net in LDM. Its output is added to the 12 skip connections and 1 middle block of U-Net in LDM. FaceR achieves restoration using the conditions  $c_t$ ,  $c_l$ ,  $c_f$ . Here,  $c_t$  is a semantic prompt encoded using the CLIP text encoder [26] (e.g., "a human face"), which is input into LDM. We pass the retouching label  $\mathbf{m}_l$  (e.g., [1,0,3] representing the degrees of eye enlarging, face lifting, and smoothing, respectively) through fully connected layers to obtain an embedding  $c_l$ , with a shape of  $3 \times 768$  dimensions, the process of the MLP is as follows:

$$c_l = \text{MLP}(\mathbf{m}_l) = \text{reshape}(\mathbf{m}_l \cdot \mathbf{W}, [-1, 3, 768]), \quad (4)$$

where  $\mathbf{W}$  is the weight matrix of the fully connected layer.  $c_f$  represents the retouched image in the latent space, obtained by encoding the latent code  $\mathcal{E}(x_0)$  using zero convolution layers. The process

of the zero convolution layers is as follows:

$$c_f = \mathcal{Z}(\mathcal{E}(x_0); \Theta), \quad (5)$$

where  $\mathcal{Z}(\cdot; \cdot)$  denotes the zero convolution layers, and  $\Theta$  represents its parameters. In the ControlNet component of FaceR,  $c_l$  and  $c_f$  are used as inputs, while in the LDM component,  $c_t$  is used as input. Additionally, noise maps are input into both parts. After processing through FaceR, the latent representation  $c_f$  results in the restored image  $y$ .

### 3.3 Hierarchical Adaptive Instance Normalization

---

#### Algorithm 1: Hierarchical Adaptive Instance Normalization

---

**Input:**

- hierarchical level  $L$ ,
- retouched image  $x \in \mathbb{R}^{C \times H \times W}$ ,
- restored image  $y \in \mathbb{R}^{C \times H \times W}$ ,
- overlapping ratio  $\gamma$ .

**Output:** corrected result  $\hat{y}$

```

1  $\hat{y}^{(L)} = y$ 
2 for  $l = L$  to 1 do
3    $H_p = \lceil \frac{H}{(1+(l-1) \times (1-\gamma))} \rceil$ 
4    $W_p = \lceil \frac{W}{(1+(l-1) \times (1-\gamma))} \rceil$ 
5    $x_p^{(l)} = \text{Patchify}(x, H_p, W_p, \gamma) \in \mathbb{R}^{N_p \times C \times H_p \times W_p}$ 
6    $\hat{y}_p^{(l)} = \text{Patchify}(\hat{y}^{(l)}, H_p, W_p, \gamma) \in \mathbb{R}^{N_p \times C \times H_p \times W_p}$ 
7   for  $i = 0$  to  $N_p$  do
8      $\tilde{y}_p^{(l)}[i] = \text{AdaIN}(\hat{y}_p^{(l)}[i], x_p^{(l)}[i]) \in \mathbb{R}^{C \times H_p \times W_p}$ 
9   end
10   $\hat{y}^{(l-1)} = \text{DePatchify}(\tilde{y}_p^{(l)}, H, W, \gamma) \in \mathbb{R}^{C \times H \times W}$ 
11 end
12  $\hat{y} = \hat{y}^{(0)}$ 
13 return  $\hat{y}$ 

```

---

Diffusion models often exhibit strong generative capabilities but are frequently plagued by color shifts [6]. To address the color mismatch issue between the restored image and the input conditional image, a straightforward approach is to employ adaptive instance normalization (AdaIN) [36]. Specifically, let  $x \in \mathbb{R}^{C \times H \times W}$  denote the input image to FaceR and  $y \in \mathbb{R}^{C \times H \times W}$  represent the restored image from FaceR. Then the calculation formula for AdaIN can be expressed as:

$$\hat{y}^c = \text{AdaIN}(x, y) = \mu_x^c + \sigma_x^c \frac{(y^c - \mu_y^c)}{\sigma_y^c}, \quad (6)$$

where  $\mu$  and  $\sigma$  represent estimated mean and standard deviation, respectively, and  $c \in \{R, G, B\}$  denotes the three color channels. AdaIN performs global consistent scaling and shifting of all pixel values by computing the statistical features of the input and output images. Although this simple global color correction technique can mitigate color discrepancies between the generated images and input images to a certain extent, when encountering complex

backgrounds or accessories around the face, the generated images by the restoration network exhibit not only simple global color shifts but also varying degrees of color shifts in different image regions. As illustrated in Figure 5, row 1, column 3, under these circumstances, AdaIN is unable to faithfully restore the color of the earring.

To address the aforementioned new issue, we further propose Hierarchical Adaptive Instance Normalization (H-AdaIN), as illustrated in Fig. 3. We perform different levels of overlapping patchification on the retouched image  $\mathbf{x}$  and the initial generated image  $\mathbf{y}$  simultaneously. At each level  $l$ , from  $\mathbf{x}$  and  $\mathbf{y}^{(l)}$ , we find the corresponding pair of patches  $(\mathbf{x}_i, \mathbf{y}_i^{(l)})$ , which are fed into AdaIN. The overall process order is from the finest level  $L$  to the coarsest level 1. The details of H-AdaIN can be referred to Algo. 1.

### 3.4 Training Strategy

For the entire Face2Face framework, we employ a strategy of decoupled training, training the Facial Retouching Detector and FaceR separately. Note that the training of the MLP is included within FaceR. The training of the Facial Retouching Detector followed the method outlined in [41], utilizing ground-truth retouching labels paired with retouched images from the RetouchingFFHQ training set for training. For the training of FaceR, we provide ground-truth retouching labels, retouched images, and ground-truth unretouched images for training. The parameters of the LDM module are frozen, and only the ControlNet part is trained. To enable FaceR to effectively align the semantic information of facial features with retouching labels, we adopt an efficient method by dividing the conditions  $\mathbf{c}_t, \mathbf{c}_l, \mathbf{c}_f$  into two distinct groups. One group utilizes the text-to-image prior from a pre-trained LDM model ( $\mathbf{c}_t \rightarrow \mathbf{z}_t$ ), while the other group consists of conditions that need to be learned from the dataset: image-to-image ( $\mathbf{c}_f \rightarrow \mathbf{z}_t$ ) and label-to-image ( $\mathbf{c}_l \rightarrow \mathbf{z}_t$ ). This separating strategy prevents knowledge from forgetting in the pre-trained diffusion model. By providing the conditions from the retouching label embedding  $\mathbf{c}_l$ , it effectively reduces the uncertainty in estimating  $p(\mathbf{c}_f | \mathbf{z}_t, \mathbf{c}_l)$ , thereby avoiding uncontrollable blind restoration and ensuring better alignment with the original image.

Initially, the pre-trained latent diffusion U-Net,  $\epsilon_\theta(\mathbf{z}_t, t, \mathbf{c}_t)$ , remains fixed during the training process, thereby preserving the text-to-image prior,  $\nabla_{\mathbf{z}_t} \log p(\mathbf{z}_t | \mathbf{c}_t)$ . Next, we apply a ControlNet initialized with a partially pre-trained U-Net to take the feature map  $\mathbf{c}_f$  of the retouched image, and the embedding  $\mathbf{c}_l$  of the retouching label. Given the input image  $\mathbf{z}_0$ , image diffusion algorithms gradually introduce noise into the image, resulting in a noisy image  $\mathbf{z}_t$ , which is input into both the ControlNet and added to  $\mathbf{c}_f$  as well as input into the frozen U-Net. To ensure that the retouched image  $\mathbf{x}_0$  matches the shape of  $\mathbf{z}_t$  and to prevent adding noise to the network, we apply a zero convolution layer with learnable parameters on  $\mathcal{E}(\mathbf{x}_0)$ , allowing the model to perceive and adapt to the retouched image.  $\epsilon_\theta$  predicts the noise to be added to the noisy image  $\mathbf{z}_t$  as follows:

$$\mathcal{L} = \mathbb{E}_{\mathbf{z}_t, \mathbf{c}_t, \mathbf{c}_l, \mathbf{c}_f, t, \epsilon \sim \mathcal{N}(0, I)} (\|\epsilon - \epsilon_\theta(\mathbf{z}_t, t, \mathbf{c}_t, \mathbf{c}_l, \mathbf{c}_f)\|_2^2). \quad (7)$$

## 4 EXPERIMENTS

### 4.1 Implementation Details

**Training details.** We choose RetouchingFFHQ [41] as our training dataset. During training, we select 19,757 images from the training set that don't include facial occlusion, closed eyes or infants. These images cover three retouching techniques (larger eyes, slimmer face, and smoother skin) with different retouching levels (ranging from 0 to 3) and include images with single or mixed retouching operations.

The facial retouching detector DenseNet121-MAM is trained for 30 epochs on the entire RetouchingFFHQ training dataset using the Adam optimizer [21], with the learning rate of  $2 \times 10^{-4}$  for CNN-based layers and  $1 \times 10^{-5}$  for Transformer-based layers. For the FaceR, we follow the setting of vanilla ControlNet [42], using the SD V1.5. The retouched image in latent space  $\mathbf{c}_f$  and the ground-truth retouching label embedding  $\mathbf{c}_l$  are fed into ControlNet, while the semantic prompt  $\mathbf{c}_t$  ("a human face") is fed into LDM. We train FaceR with a batch size of 20 and a learning rate of  $1 \times 10^{-5}$  for 100 epochs. The training process is conducted on a single NVIDIA A800 GPU (80G) and completed within 7 days.

**Evaluation setting.** We randomly select 1000 pairs of retouched and original images with different retouching methods and levels from the RetouchingFFHQ validation set for evaluation. We set up two sets of retouching labels: ground truth and the detection results from our facial retouching detector. The restored images are then processed through the H-AdaIN module to demonstrate the effectiveness of the facial retouching detector and H-AdaIN.

### 4.2 Comparison with Other Methods

**Comparing methods.** We select four methods for comparison, including SSAT [35], InstructPix2Pix (IP2P) [3], ControlNet and ControlNet+Text. The first two are pre-existing methods without specific training on our task; the latter two are baseline methods proposed by us, which are specifically trained on our task.

Originally designed for makeup transfer, SSAT requires the provision of both a makeup-applied image and a non-makeup image. In our experiments, we supply retouched photos alongside non-retouched photos as input, seeking to enable the model to transition the subject from a "retouched" state to a "non-retouched" state. IP2P is initially intended for instruction-based image editing; in our case, we introduce retouching degrees via textual prompts. ControlNet performs the blind restoration of retouched images without any prompt. ControlNet+Text introduces the retouching degrees through textual prompts. The approach to incorporating the retouching degrees is discussed in Sec. 4.1. For methods that only support text conditions, we use text prompts instead of retouching labels. For example, "EyeEnlarging 3; FaceLifting 1; Smoothing 0" corresponds to the retouching label "[3, 1, 0]".

**Evaluation metrics.** We select several commonly used evaluation metrics for image restoration tasks, including traditional metrics such as Peak Signal-to-Noise Ratio (PSNR) and Structural Similarity Index Measure (SSIM) [38], as well as learning-based metrics, namely Learned Perceptual Image Patch Similarity (LPIPS) [43], Deep Image Structure and Texture Similarity (DISTS) [9] and Fréchet Inception Distance (FID) [13].

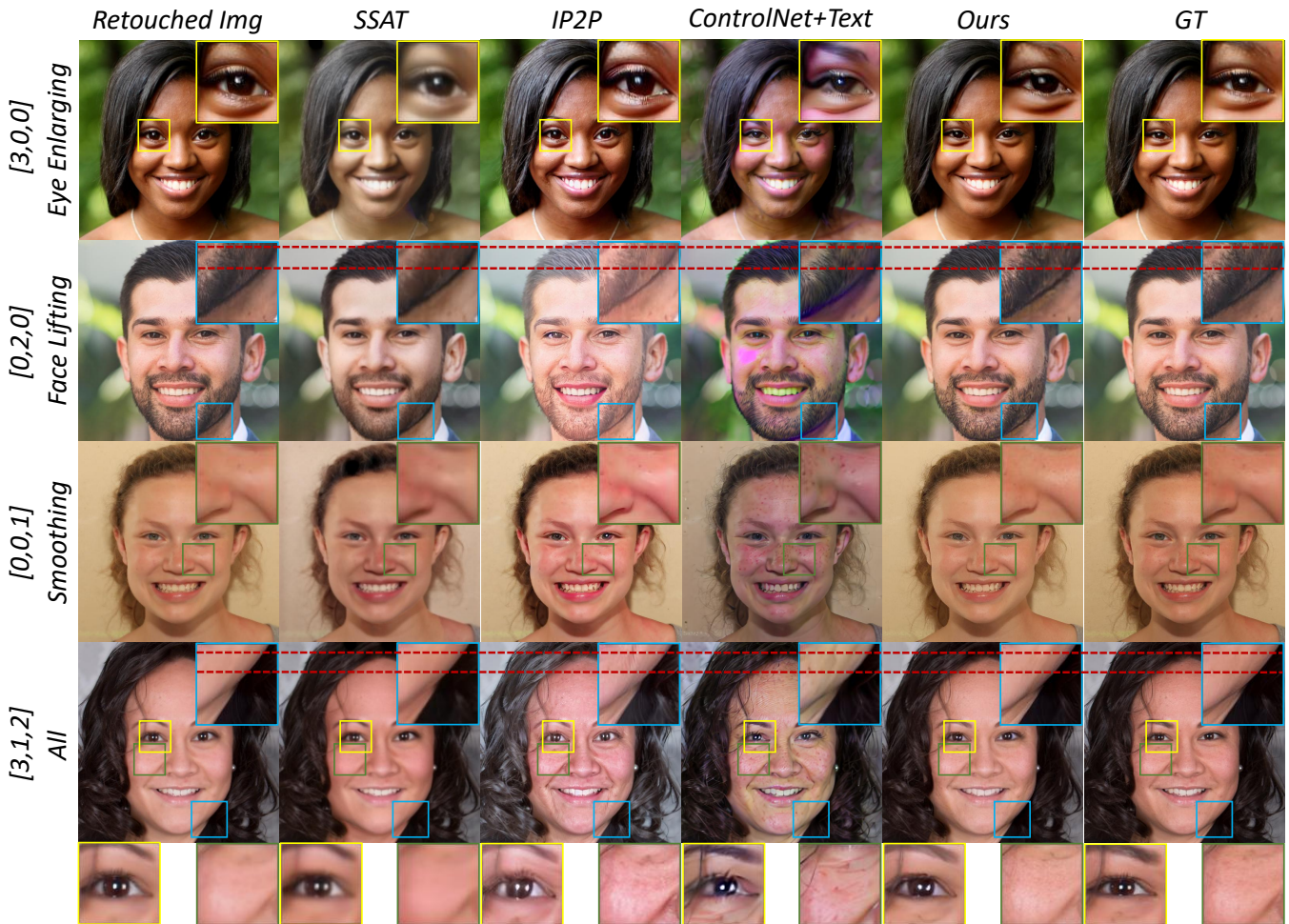


Figure 4: Visual comparison with other methods. The labels to the left of the images indicate the types and degrees of retouching, while the captions on the top indicate the different methods, ground truth, or retouched images. In particular, for ControlNet+Text, we utilize text prompts instead of ground-truth retouching labels. For instance, "EyeEnlarging 3; FaceLifting 1; Smoothing 0" corresponds to the retouching label "[3, 1, 0]". The red dashed line is convenient for observing face lifting.

**Quantitative experiments.** We present a quantitative comparison of various approaches on the RetouchingFFHQ test set. As shown in Tab. 1, our method outperforms various image-to-image methods in multiple perceptual metrics, including FID, SSIM, PSNR, LPIPS, and DISTS. Specifically, our Face2Face with detector achieves an FID score of 23.48, which is 59.43% lower than IP2P based on LDM and 71.89% lower than ControlNet+Text, and 74.16% lower than SSAT. Furthermore, our Face2Face surpasses the compared methods in the remaining metrics, indicating its superiority. The inclusion of the ground-truth label comparison in the experiment with Face2Face using a facial retouching detector aims to highlight the quality upper bound of Face2Face. It is noteworthy that although SSAT and IP2P achieve good LPIPS and DISTS scores, they exhibit poorer performance in other perceptual metrics (i.e., FID, SSIM, PSNR).

**Qualitative experiments.** We conduct qualitative tests on the RetouchingFFHQ test set to demonstrate the effectiveness of our

method, as shown in Fig. 4. It is observed that Face2Face is capable of faithfully and naturally restoring images according to the retouching labels, as illustrated in the fifth column of Fig. 4. In contrast, other approaches either exhibit no response to the instructions for retouching restoration or transform styles (as in the case of IP2P) or are capable of following the retouching label for restoration (such as ControlNet+Text) but result in unnatural coloration and details. Particularly, in the case of the smoothing operation, SSAT fails to handle this operation, whereas IP2P and ControlNet+Text, although able to identify and address smoothing, generate details that do not belong to the original image.

### 4.3 Ablation Study on H-AdaIN

To achieve optimal qualitative and quantitative results, we conduct comparative experiments on the hyperparameters involved in Hierarchical Adaptive Instance Normalization (H-AdaIN), including the hierarchical level  $L$  and overlapping ratio  $\gamma$  (See Algo. 1 for

**Table 1: Quantitative results on the RetouchingFFHQ. SSAT and IP2P are pre-existing methods without specific training on our task, while the remaining methods are specifically trained on our task. "No" indicates the absence of retouching labels, "GT" denotes the usage of real retouching labels, and "Detector" indicates the utilization of retouching labels generated through the facial retouching detector. Red and bold signify the optimal values, while blue denotes sub-optimal values.**

Method	Label	FID↓	SSIM↑	PSNR↑	LPIPS↓	DISTS↓
SSAT	No	91.30	0.8318	21.84	0.2746	0.1810
IP2P	No	58.16	0.7870	21.69	0.2073	0.0995
ControlNet	No	199.94	0.4381	21.31	0.6290	0.4395
ControlNet+Text	GT	83.95	0.7774	21.92	0.3515	0.1608
Ours w/o H-AdaIN	GT	44.83	0.8478	26.88	0.2233	0.0963
Ours w/o H-AdaIN	Detector	44.97	0.8440	26.57	0.2285	0.0979
Ours	GT	<b>23.48</b>	<b>0.8556</b>	<b>28.24</b>	<b>0.1677</b>	<b>0.0737</b>
Ours	Detector	<b>23.60</b>	<b>0.8532</b>	<b>28.19</b>	<b>0.1693</b>	<b>0.0741</b>

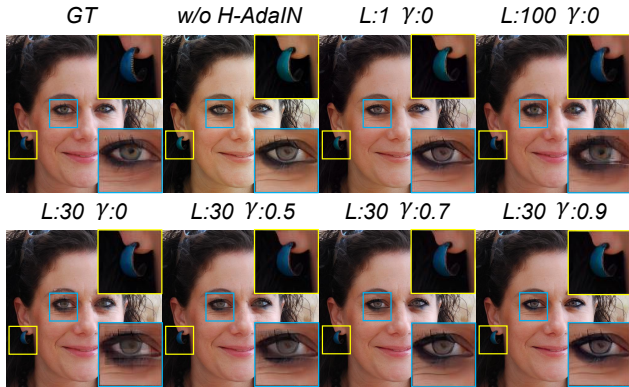


**Figure 5: The results of applying different hyperparameters to H-AdaIN, where "L" denotes hierarchical level, and "γ" represents the overlapping ratio.**

**Table 2: Ablation of H-AdaIN’s hyperparameters. We compare different hyperparameters, where setting "L" equal to 1 is equivalent to directly applying AdaIN. All experiments utilize retouching labels generated through the facial retouching detector. The final line represents the parameters we have ultimately selected. Red and bold signify the optimal values, while blue denotes sub-optimal values.**

L	γ	FID↓	SSIM↑	PSNR↑	LPIPS↓	DISTS↓
1	0	44.06	0.8385	26.09	0.2312	0.0986
30	0	23.83	0.8523	28.15	0.1742	0.0774
100	0	<b>19.71</b>	<b>0.8720</b>	<b>28.51</b>	<b>0.1550</b>	<b>0.0745</b>
30	0.5	<b>23.37</b>	0.8514	28.16	0.1723	0.0752
30	0.9	30.99	0.8501	27.76	0.1862	0.0851
30	0.7	23.60	<b>0.8532</b>	<b>28.19</b>	<b>0.1693</b>	<b>0.0741</b>

the details of algorithm and parameters). The hierarchical level  $L$  determines the maximum number of patches segmented from the original image, whereas the overlapping ratio  $\gamma$  governs the

proportion of edges that overlap between adjacent patches. As a control, we also present the results when not utilizing H-AdaIN and when solely employing AdaIN (wherein H-AdaIN degrades into AdaIN when the parameter  $L$  is set to 1).

Our qualitative and quantitative results are exhibited in Fig. 5 and Tab. 2. Firstly, we determine the optimal value of  $L$  when  $\gamma$  is 0; then with the optimal value of  $L$  set to 30, we determine the optimal value of  $\gamma$ .

When only AdaIN is used (i.e.  $L=1$ ), the earring appears green as opposed to the ground truth of the blue, indicating that the color is not faithfully restored. The first row of Tab. 2 further reveals that the quantitative outcomes derived solely from AdaIN are sub-optimal. With  $L$  set to 100, although the earring’s color is faithfully restored and the quantitative results surpass all other comparative experiments, an erroneous enlargement of small eyes is discernible in Fig. 5 as generated by the restoration network. We hypothesize as follows: given that the restoration network is tasked with reverting images retouched to showcase larger eyes, certain pixels that belong to the eyes before restoration do not after; thus when  $L$  is excessively large, H-AdaIN extracts pixel information from small patches that are initially part of the eye and erroneously applies it to patches that are not part of the eye post-restoration, leading to the undesired magnification of the eye region. Consequently, for  $L$ , a moderate value of 30 is selected.

Tab. 2 reveals that when  $L$  is set to 30 and  $\gamma$  is less than 0.9, the differences in quantitative results are negligible. However, additional insights can be gleaned from Fig. 5. When  $\gamma$  is too small, due to the lack of overlap in the processing of adjacent patches, conspicuous patch boundaries are apparent within the image. Conversely, when  $\gamma$  is too large, H-AdaIN tends towards the behavior of AdaIN, thus experiencing similar issues with AdaIN – non-faithful color restoration. Ultimately, for  $\gamma$ , a moderate value of 0.7 is chosen.

## 5 CONCLUSION

We propose a retouching-label-driven framework for the restoration of retouched facial images. To the best of our knowledge, this is the first framework supporting the restoration of retouched images involving deformations. In addition, we propose a color correction module, Hierarchical Adaptive Instance Normalization (H-AdaIN),

to address the issue of color shift. Extensive experiments demonstrate that our approach outperforms previous methods significantly in both qualitative and quantitative results. Our framework establishes a new paradigm for retouched image restoration, paving the way for further developments.

**Limitations.** As an initial effort to restore facial deformation retouching manipulations, our research is confined to three prevalent retouching techniques. The undertaking to restore a more extensive array of retouching methods is left for future work. Additionally, our approach still falls short of fully restoring retouched images to the exact level of the original images. Precisely controlling the degree of restoration in cases involving deformations remains a significant challenge. Meanwhile, the detection of retouching methods and their degree remains somewhat inaccurate, especially in cases where images undergo multiple types of retouching.

## REFERENCES

- [1] Aparna Bharati, Richa Singh, Mayank Vatsa, and Kevin W Bowyer. 2016. Detecting facial retouching using supervised deep learning. *IEEE Transactions on Information Forensics and Security* 11, 9 (2016), 1903–1913.
- [2] Andrew Brock, Jeff Donahue, and Karen Simonyan. 2019. Large Scale GAN Training for High Fidelity Natural Image Synthesis. arXiv:1809.11096 [cs.LG]
- [3] Tim Brooks, Aleksander Holynski, and Alexei A. Efros. 2023. InstructPix2Pix: Learning To Follow Image Editing Instructions. In *Proceedings of the IEEE/CVF Conference on Computer Vision and Pattern Recognition (CVPR)*. 18392–18402.
- [4] Ying-Cong Chen, Xiaoyong Shen, and Jiaya Jia. 2017. Makeup-go: Blind reversion of portrait edit. In *Proceedings of the IEEE International Conference on Computer Vision*. 4501–4509.
- [5] Ying-Cong Chen, Xiaogang Xu, and Jiaya Jia. 2020. Domain Adaptive Image-to-Image Translation. In *Proceedings of the IEEE/CVF Conference on Computer Vision and Pattern Recognition (CVPR)*.
- [6] Jooyoung Choi, Jungbeom Lee, Chaehun Shin, Sungwon Kim, Hyunwoo Kim, and Sungroh Yoon. 2022. Perception prioritized training of diffusion models. In *Proceedings of the IEEE/CVF Conference on Computer Vision and Pattern Recognition*. 11472–11481.
- [7] Antitza Dantcheva, Cunjian Chen, and Arun Ross. 2012. Can facial cosmetics affect the matching accuracy of face recognition systems?. In *2012 IEEE Fifth international conference on biometrics: theory, applications and systems (BTAS)*. IEEE, 391–398.
- [8] Prafulla Dhariwal and Alexander Nichol. 2021. Diffusion models beat gans on image synthesis. *Advances in neural information processing systems* 34 (2021), 8780–8794.
- [9] Keyan Ding, Kede Ma, Shiqi Wang, and Eero P Simoncelli. 2020. Image quality assessment: Unifying structure and texture similarity. *IEEE transactions on pattern analysis and machine intelligence* 44, 5 (2020), 2567–2581.
- [10] Rinon Gal, Yuval Alaluf, Yuval Atzmon, Or Patashnik, Amit H. Bermano, Gal Chechik, and Daniel Cohen-Or. 2022. An Image is Worth One Word: Personalizing Text-to-Image Generation using Textual Inversion. arXiv:2208.01618 [cs.CV]
- [11] Mengyue Geng, Peixi Peng, Yangru Huang, and Yonghong Tian. 2020. Masked face recognition with generative data augmentation and domain constrained ranking. In *Proceedings of the 28th ACM international conference on multimedia*. 2246–2254.
- [12] Qiao Gu, Guanzhi Wang, Mang Tik Chiu, Yu-Wing Tai, and Chi-Keung Tang. 2019. Ladrn: Local adversarial disentangling network for facial makeup and de-makeup. In *Proceedings of the IEEE/CVF International conference on computer vision*. 10481–10490.
- [13] Martin Heusel, Hubert Ramsauer, Thomas Unterthiner, Bernhard Nessler, and Sepp Hochreiter. 2017. Gans trained by a two time-scale update rule converge to a local nash equilibrium. *Advances in neural information processing systems* 30 (2017).
- [14] Jonathan Ho, Ajay Jain, and Pieter Abbeel. 2020. Denoising diffusion probabilistic models. *Advances in neural information processing systems* 33 (2020), 6840–6851.
- [15] Jonathan Ho and Tim Salimans. 2022. Classifier-Free Diffusion Guidance. arXiv:2207.12598 [cs.LG]
- [16] Gao Huang, Zhuang Liu, Laurens Van Der Maaten, and Kilian Q Weinberger. 2017. Densely connected convolutional networks. In *Proceedings of the IEEE conference on computer vision and pattern recognition*. 4700–4708.
- [17] Xun Huang and Serge Belongie. 2017. Arbitrary Style Transfer in Real-Time With Adaptive Instance Normalization. In *Proceedings of the IEEE International Conference on Computer Vision (ICCV)*.
- [18] Anubhav Jain, Puspita Majumdar, Richa Singh, and Mayank Vatsa. 2020. Detecting GANs and retouching based digital alterations via DAD-HCNN. In *Proceedings of the IEEE/CVF Conference on Computer Vision and Pattern Recognition Workshops*. 672–673.
- [19] Anubhav Jain, Richa Singh, and Mayank Vatsa. 2018. On detecting GANs and retouching based synthetic alterations. In *2018 IEEE 9th international conference on biometrics theory, applications and systems (BTAS)*. IEEE, 1–7.
- [20] Eric Jang, Shixiang Gu, and Ben Poole. 2017. Categorical Reparameterization with Gumbel-Softmax. arXiv:1611.01144 [stat.ML]
- [21] Diederik P. Kingma and Jimmy Ba. 2017. Adam: A Method for Stochastic Optimization. arXiv:1412.6980 [cs.LG]
- [22] Nupur Kumari, Bingliang Zhang, Richard Zhang, Eli Shechtman, and Jun-Yan Zhu. 2023. Multi-concept customization of text-to-image diffusion. In *Proceedings of the IEEE/CVF Conference on Computer Vision and Pattern Recognition*. 1931–1941.
- [23] Tingting Li, Ruihe Qian, Chao Dong, Si Liu, Qiong Yan, Wenwu Zhu, and Liang Lin. 2018. Beautygan: Instance-level facial makeup transfer with deep generative adversarial network. In *Proceedings of the 26th ACM international conference on Multimedia*. 645–653.
- [24] Si Liu, Wentao Jiang, Chen Gao, Ran He, Jiashi Feng, Bo Li, and Shuicheng Yan. 2021. Psgan++: Robust detail-preserving makeup transfer and removal. *IEEE Transactions on Pattern Analysis and Machine Intelligence* 44, 11 (2021), 8538–8551.
- [25] Chong Mou, Xintao Wang, Liangbin Xie, Yanze Wu, Jian Zhang, Zhongang Qi, and Ying Shan. 2024. T2i-adapter: Learning adapters to dig out more controllable ability for text-to-image diffusion models. In *Proceedings of the AAAI Conference on Artificial Intelligence*, Vol. 38. 4296–4304.
- [26] Alec Radford, Jong Wook Kim, Chris Hallacy, Aditya Ramesh, Gabriel Goh, Sandhini Agarwal, Girish Sastry, Amanda Askell, Pamela Mishkin, Jack Clark, et al. 2021. Learning transferable visual models from natural language supervision. In *International conference on machine learning*. PMLR, 8748–8763.
- [27] Christian Rathgeb, Angelika Botalov, Fabian Stockhardt, Sergey Isadskiy, Luca DeBiasi, Andreas Uhl, and Christoph Busch. 2020. PRNU-based detection of facial retouching. *IET Biometrics* 9, 4 (2020), 154–164.
- [28] Christian Rathgeb, C-I Satnoianu, Nathania E Haryanto, Kevin Bernardo, and Christoph Busch. 2020. Differential detection of facial retouching: A multi-biometric approach. *IEEE Access* 8 (2020), 106373–106385.
- [29] Christian Rathgeb, Ruben Tolosana, Ruben Vera-Rodriguez, and Christoph Busch. 2022. *Handbook of digital face manipulation and detection: from DeepFakes to morphing attacks*. Springer Nature.
- [30] Robin Rombach, Andreas Blattmann, Dominik Lorenz, Patrick Esser, and Björn Ommer. 2022. High-resolution image synthesis with latent diffusion models. In *Proceedings of the IEEE/CVF conference on computer vision and pattern recognition*. 10684–10695.
- [31] Olaf Ronneberger, Philipp Fischer, and Thomas Brox. 2015. U-net: Convolutional networks for biomedical image segmentation. In *Medical image computing and computer-assisted intervention—MICCAI 2015: 18th international conference, Munich, Germany, October 5–9, 2015, proceedings, part III 18*. Springer, 234–241.
- [32] Olga Russakovsky, Jia Deng, Hao Su, Jonathan Krause, Sanjeev Satheesh, Sean Ma, Zhiheng Huang, Andrej Karpathy, Aditya Khosla, Michael Bernstein, et al. 2015. Imagenet large scale visual recognition challenge. *International journal of computer vision* 115 (2015), 211–252.
- [33] Kamal Sharma, Gurinder Singh, and Puneet Goyal. 2023. IPDCN2: Improved Patch-based Deep CNN for facial retouching detection. *Expert Systems with Applications* 211 (2023), 118612.
- [34] Yang Song, Jascha Sohl-Dickstein, Diederik P. Kingma, Abhishek Kumar, Stefano Ermon, and Ben Poole. 2021. Score-Based Generative Modeling through Stochastic Differential Equations. arXiv:2011.13456 [cs.LG]
- [35] Zhaoyang Sun, Yaxiong Chen, and Shengwu Xiong. 2022. Ssat: A symmetric semantic-aware transformer network for makeup transfer and removal. In *Proceedings of the AAAI Conference on artificial intelligence*, Vol. 36. 2325–2334.
- [36] Jianyi Wang, Zongsheng Yue, Shangchen Zhou, Kelvin C. K. Chan, and Chen Change Loy. 2023. Exploiting Diffusion Prior for Real-World Image Super-Resolution. arXiv:2305.07015 [cs.CV]
- [37] Tengfei Wang, Ting Zhang, Bo Zhang, Hao Ouyang, Dong Chen, Qifeng Chen, and Fang Wen. 2022. Pretraining is All You Need for Image-to-Image Translation. arXiv:2205.12952 [cs.CV]
- [38] Zhou Wang, Alan C Bovik, Hamid R Sheikh, and Eero P Simoncelli. 2004. Image quality assessment: from error visibility to structural similarity. *IEEE transactions on image processing* 13, 4 (2004), 600–612.
- [39] Zeheng Wang, Zitong Yu, Chenxu Zhao, Xiangyu Zhu, Yunxiao Qin, Qiusheng Zhou, Feng Zhou, and Zhen Lei. 2020. Deep spatial gradient and temporal depth learning for face anti-spoofing. In *Proceedings of the IEEE/CVF conference on computer vision and pattern recognition*. 5042–5051.
- [40] Shuai Yang, Yifan Zhou, Ziwei Liu, and Chen Change Loy. 2023. Rerender A Video: Zero-Shot Text-Guided Video-to-Video Translation. In *SIGGRAPH Asia 2023 Conference Papers* (<conf-loc>, <city>Sydney</city>, <state>NSW</state>, <country>Australia</country>, </conf-loc>) (SA '23). Association for Computing

- Machinery, New York, NY, USA, Article 95, 11 pages. <https://doi.org/10.1145/3610548.3618160>
- [41] Qichao Ying, Jiaxin Liu, Sheng Li, Haisheng Xu, Zhenxing Qian, and Xinpeng Zhang. 2023. RetouchingFFHQ: A Large-scale Dataset for Fine-grained Face Retouching Detection. In *Proceedings of the 31st ACM International Conference on Multimedia*. 737–746.
- [42] Lvmin Zhang, Anyi Rao, and Maneesh Agrawala. 2023. Adding conditional control to text-to-image diffusion models. In *Proceedings of the IEEE/CVF International Conference on Computer Vision*. 3836–3847.
- [43] Richard Zhang, Phillip Isola, Alexei A Efros, Eli Shechtman, and Oliver Wang. 2018. The unreasonable effectiveness of deep features as a perceptual metric. In *Proceedings of the IEEE conference on computer vision and pattern recognition*. 586–595.